

## GROWING $\text{Sb}_2\text{Se}_3$ FILMS ENRICHED WITH SELENIUM USING CHEMICAL MOLECULAR BEAM DEPOSITION

 Takhirdjon M. Razikov,  Sultanpasha A. Muzafarova\*,  Ruhiddin T. Yuldoshov\*,  
 Zafarjon M. Khusanov, Marg'uba K. Khusanova, Z.S. Kenzhaeva, B.V. Ibragimova

*Institute of Semiconductor Physics and Microelectronics at the National University of Uzbekistan,  
20 Yangi Almazar St., Tashkent, 100057, Uzbekistan*

*\*Corresponding Author e-mail: [samusu@rambler.ru](mailto:samusu@rambler.ru); [ruhiddin@yahoo.com](mailto:ruhiddin@yahoo.com)*

Received January 2, 2024; revised January 22, 2024; accepted February 15, 2024

This study explores the growth of  $\text{Sb}_2\text{Se}_3$  films on soda-lime glass (SLG) surfaces using the chemical molecular beam deposition (CMPD) method at a substrate temperature of 500°C. High-purity binary compounds,  $\text{Sb}_2\text{Se}_3$  and Se, were employed as source materials for film deposition. Scanning electron microscopy (SEM) was employed to investigate the morphological characteristics of the  $\text{Sb}_2\text{Se}_3$  films. Furthermore, the influence of temperature on the grain size and crystallographic orientation in selenium films was examined. Samples were obtained from a selenium source at temperatures of 370°C and 430°C. The results indicate that increasing the temperature of the selenium source results in the formation of larger grains and the presence of rod-shaped grains of  $\text{Sb}_2\text{Se}_3$  aligned parallel to the substrate. A sample obtained at 370°C exhibited grains larger than 2  $\mu\text{m}$  in size, evenly distributed across the substrate surface, indicating a uniform growth process. In contrast, when the temperature of the selenium source was raised to 430°C, considerably larger grains measuring approximately 4  $\mu\text{m}$  were detected on the film surface substrate. X-ray diffraction analysis was conducted to gain insights into the crystalline phases and crystal structure of the  $\text{Sb}_2\text{Se}_3$  films synthesized under different temperatures of the selenium source. The X-ray diffraction patterns displayed prominent peaks corresponding to the crystallographic planes (221) and (211), indicating the presence of strong crystalline phases. Additionally, peaks such as (020), (120), and (310) were observed in the X-ray patterns, further confirming the crystallinity of the films.

**Keywords:** *X-ray diffraction; Chemical molecular beam deposition;  $\text{Sb}_2\text{Se}_3$ ; Selenium temperature*

**PACS:** 73.22

### 1. INTRODUCTION

Antimony selenide ( $\text{Sb}_2\text{Se}_3$ ) has emerged as one of the most promising absorber materials for the development of next-generation thin-film solar cells, due to its outstanding photovoltaic performance. The remarkable properties of  $\text{Sb}_2\text{Se}_3$ , including its simple crystal structure, substantial absorption coefficient exceeding  $10^5 \text{ cm}^{-1}$ , ideal band gap within the 1.1–1.3 eV range, and significant mobility, approximately  $10 \text{ cm}^2\text{V}^{-1}\text{s}^{-1}$  [1], make it a highly attractive candidate for advanced thin-film solar cells. One distinct advantage of  $\text{Sb}_2\text{Se}_3$ , compared to more established thin-film solar cells, specifically Copper Indium Gallium Selenide ( $\text{CuInGaSe(S)}_4$ , referred to as CIGS) and Cadmium Telluride (CdTe), is its cost-effectiveness. Both antimony (Sb) and selenium (Se), the constituent elements of  $\text{Sb}_2\text{Se}_3$ , are widely available and exhibit lower toxicity. As such, we can anticipate that  $\text{Sb}_2\text{Se}_3$  technology will become a serious competitor in the mass production of thin-film photovoltaic modules. It has been discovered that [hk1]-oriented (vertically oriented)  $\text{Sb}_2\text{Se}_3$  film is superior for efficient charge carrier transfer compared to the [hk0]-oriented  $\text{Sb}_2\text{Se}_3$  compound film. However, controlling the orientation of the thin film remains a significant hurdle to further enhancing the efficiency of  $\text{Sb}_2\text{Se}_3$ -based solar cells. It should be noted that during the synthesis of  $\text{Sb}_2\text{Se}_3$  films via physical methods, a considerable amount of Se is lost due to film decomposition into Sb, Se, and SbSe. This results in the formation of Se vacancies, which subsequently increase the density of recombination centers in the films [2]. These changes have a negative impact on the optical and electrophysical properties of the solar cells. To mitigate this issue, researchers propose additional heat treatment in Se vapor. Zhiqiang Lee [2] has successfully produced thin film  $\text{Sb}_2\text{Se}_3$  using a co-evaporation method of  $\text{Sb}_2\text{Se}_3$  and Se [3, 4], whilst Shongalova [5] has introduced a method for creating  $\text{Sb}_2\text{Se}_3$  films by sputtering, followed by "selenized" annealing in a  $\text{H}_2\text{Se}$  gas atmosphere. These innovative solutions illustrate the ongoing advancements in the field, paving the way for the full realization of  $\text{Sb}_2\text{Se}_3$  potential in next-generation solar technology.

$\text{Sb}_2\text{Se}_3$  films are used various methods precipitation: thermal evaporation [6-7], gas transport evaporation [8, 9] method sublimation in a closed vacuum [10] and magnetron sputtering [11]. In this work, first time to grows films  $\text{Sb}_2\text{Se}_3$  for solar cells by chemical molecular beam deposition (CMBD) method. In this study, we investigate the growth of  $\text{Sb}_2\text{Se}_3$  films on SLG substrates using the CMBD method.

### 2. MATERIALS AND METHODS

Installed technological mode optimal grow  $\text{Sb}_2\text{Se}_3$  films on surfaces SLG (soda- lime glass ) by the method chemical molecular beam precipitation (Fig. 1). The experimental system was prepared by purging hydrogen to eliminate atmospheric pollutants. The SLG substrates with dimensions of  $2.0 \times 2.0 \text{ cm}^2$  were used for film deposition. To obtain  $\text{Sb}_2\text{Se}_3$  films with enriched selenium content and stoichiometric composition, the partial pressure of Se in the steam phase was adjusted during

the growth process. The substrate temperature was maintained at  $500^\circ\text{C}$ , while the temperatures of the source elements were varied within the ranges of  $350^\circ\text{C}$  to  $430^\circ\text{C}$  for Se and  $700^\circ\text{C}$  for  $\text{Sb}_2\text{Se}_3$ . The growth rate was controlled between  $0.1$  to  $1 \text{ \AA}/\text{sec}$ , and a hydrogen flow rate of  $\text{WH}_2 = 20 \text{ cm}^3/\text{min}$  was maintained.

Granules of  $\text{Sb}_2\text{Se}_3$  and high-purity Se (99.999%) were utilized as the source materials. These compounds were placed in separate containers within the experimental setup. The morphological properties of the films were examined using a scanning electron microscope (SEM-EVO MA 10). The film compositions were determined by energy-dispersive elemental analysis (EDX) using an Oxford Instrument Aztec Energy Advanced X-act SDD detector. The crystal structure and phase composition were analyzed using X-ray diffraction (XRD) with a Panalytical Empyrean diffract meter, employing  $\text{CuK}\alpha$  radiation ( $\lambda = 1.5418 \text{ \AA}$ ) and  $2\theta$  measurements in the range of  $20^\circ$  to  $80^\circ$  with a step size of  $0.01^\circ$ . The phase composition analysis was conducted using the Joint Committee on Powder Diffraction Standards (JCPDS) database.

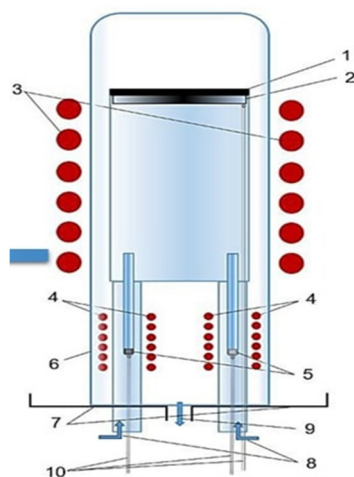


**Figure 1.** a) Schematic diagram of the system; b) Schematic image method chemical molecular beam deposition 1, 2 – substrate and its holder, 3- heater substrates, 4- heaters sources, 5- sources evaporated component ( $\text{Sb}_2\text{Se}_3$  and Se), 6- hydrogen gas carriers ( $\text{H}_2$ ), 7- flange holder, 8- hydrogen inlet, 9- hydrogen outlet, 10- thermocouple

### 3. RESULTS AND DISCUSSION

**Morphological properties.** The obtained SEM images revealed the morphological characteristics of the  $\text{Sb}_2\text{Se}_3$  films, while the EDX analysis confirmed their elemental composition.

This study investigates the influence of temperature on grain size and crystallographic orientation in selenium films. A sample was obtained from a selenium source at temperatures of  $370^\circ\text{C}$  and  $430^\circ\text{C}$ . The characterization of the samples was performed using microscopy techniques, and the results were analyzed to understand the relationship between temperature and the observed grain size and crystallographic orientation. Our findings indicate that increasing the temperature of the selenium source leads to the formation of larger grains and the presence of rod-shaped grains of  $\text{Sb}_2\text{Se}_3$  aligned parallel to the substrate. These observations are consistent with the collected data, which also revealed an increase in the peak texture coefficients ( $hk0$ ) at the temperature of  $430^\circ\text{C}$ .

Upon analyzing the sample obtained at  $370^\circ\text{C}$ , grains larger than  $2 \mu\text{m}$  in size were observed. These grains exhibited a uniform distribution across the substrate surface, indicating a uniform growth process. However, when the temperature of the selenium source was raised to  $430^\circ\text{C}$ , considerably larger grains measuring approximately  $4 \mu\text{m}$  were detected on the film surface substrate. The increase in temperature led to the formation of larger grains, which can be attributed to enhanced diffusion and coalescence processes during film growth.

Furthermore, rod-shaped grains of  $\text{Sb}_2\text{Se}_3$  were observed in the sample obtained at  $430^\circ\text{C}$ . These grains aligned themselves parallel to the substrate, as depicted in Figure 2. The formation of  $\text{Sb}_2\text{Se}_3$  grains can be attributed to the reaction between antimony (Sb) impurities present in the selenium source and the substrate material. The alignment of these rod-shaped grains suggests an epitaxial growth mechanism on the substrate surface.

The XRD analysis revealed that the peak texture coefficients ( $hk0$ ) began to exhibit an increase at the temperature of  $430^\circ\text{C}$ . This finding indicates a preferential crystallographic orientation in the film, which can be attributed to the growth conditions and the interaction between the deposited selenium and the substrate material. The increased peak texture coefficients further support the observed larger grain size and the presence of  $\text{Sb}_2\text{Se}_3$  rod-shaped grains.

These observations are consistent with our data, as the presence of larger grains can positively impact the performance of solar cells by reducing recombination losses. Larger grains tend to have fewer defects along their boundaries, which can lead to improved efficiency in converting solar energy. In conclusion, our results demonstrate that temperature influences grain size and texture in the selenium film. The larger grain size observed at higher temperatures suggests the potential for enhanced solar cell performance.

Table 1 presents the chemical composition of the elements in the deposited  $\text{Sb}_2\text{Se}_3$  films. The analysis using an energy dispersive elemental analyzer revealed that the Sb/Se atomic concentration ratio decreased as the selenium

temperature increased from 350°C to 430°C, approaching the stoichiometric composition of Sb/Se≈0.66. This indicates that the selenium content in the Sb<sub>2</sub>Se<sub>3</sub> thin films increased with higher selenium flow. At a selenium source temperature of 350°C, the Sb<sub>2</sub>Se<sub>3</sub> film was selenium-poor. However, at higher temperatures, the compound films approached a stoichiometric composition with an Sb/Se ratio of 0.68, which was achieved at a selenium source temperature of 430°C. It is evident that the temperature of the selenium source plays an important role in obtaining high-quality Sb<sub>2</sub>Se<sub>3</sub> films.

Stoichiometric, vertically oriented Sb<sub>2</sub>Se<sub>3</sub> grains larger than 4 μm were successfully obtained at a selenium temperature of 430°C, which are considered beneficial for charge carrier transport.

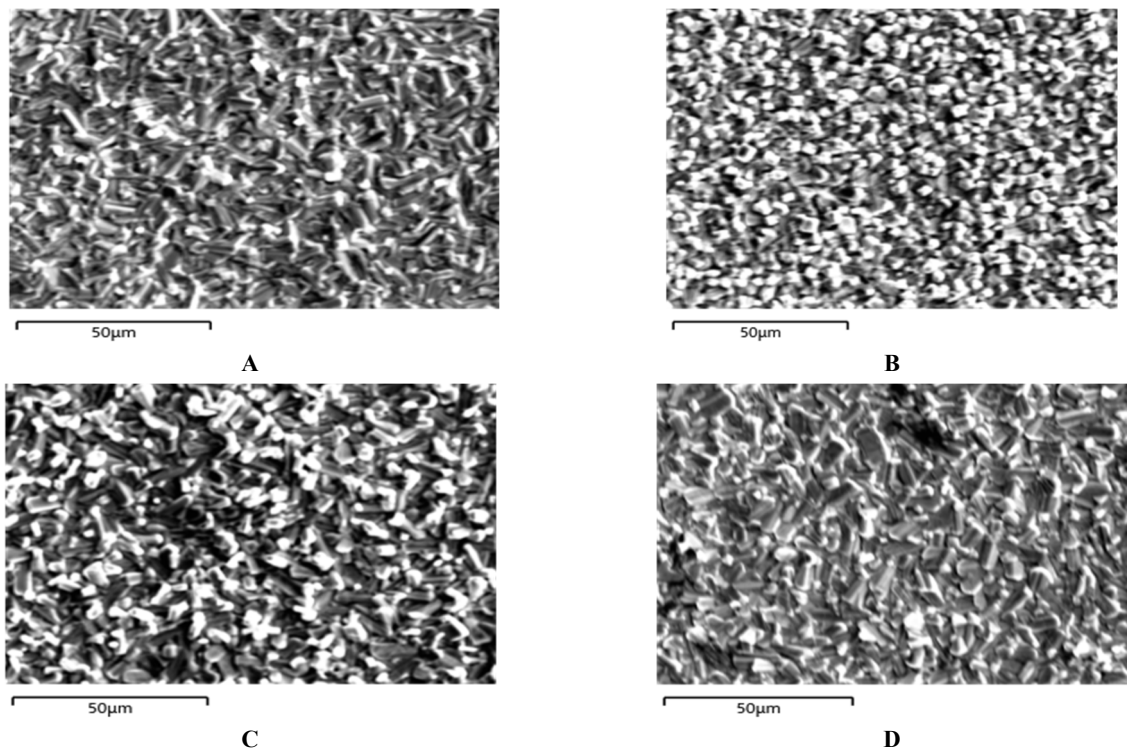


**Figure 2.** SEM images of Sb<sub>2</sub>Se<sub>3</sub> films at different selenium temperatures: a) 350°C; b) 370°C; c) 400 °C; d) 430°C

It is worth noting that Sb<sub>2</sub>Se<sub>3</sub> films exhibit p-type conductivity. However, some samples of Sb<sub>2</sub>Se<sub>3</sub> may exhibit n-type conductivity due to the presence of Sb impurities. Additionally, the presence of (V<sub>Se</sub>) defects can also contribute to n-type conductivity or act as donors [12].

**Table 1.** Chemical compound Sb<sub>2</sub>Se<sub>3</sub> films at various temperatures selenium source

T <sub>Se</sub> , (Temperatures of Selenium source °C)	T <sub>substrate</sub> , °C	weight percentage, %		Atomic percentage, %		Sb/Se
		Sb	Se	Sb	Se	
350	500	53.3	46.7	0.43	0.59	0.74
370	500	52.6	47.4	0.43	0.60	0.72
400	500	51.8	48.2	0.42	0.61	0.70
430	500	51.2	48.8	0.42	0.618	0.68

The implications of the Sb/Se atomic concentration ratio approaching the stoichiometric composition in Sb<sub>2</sub>Se<sub>3</sub> films are significant. The stoichiometric composition represents the ideal ratio of antimony (Sb) to selenium (Se) atoms in Sb<sub>2</sub>Se<sub>3</sub>. When the Sb/Se ratio approaches this stoichiometric composition, the film exhibits optimal electrical properties. This means that the film is more likely to have the desired characteristics for its intended applications, such as solar cells. Achieving the stoichiometric composition helps in attaining the desired electronic band structure and charge transport properties. Reduced Defects: Deviations from the stoichiometric composition can introduce defects in the crystal structure of the material. By approaching the stoichiometric composition, the number of defects, such as vacancies or impurities, can be minimized. Fewer defects lead to improved electrical and optical properties, as defects act as recombination centers for charge carriers, reducing their lifetime and overall device performance.

**Structural properties of Sb<sub>2</sub>Se<sub>3</sub> films.** Figure 3 present the outcomes of the X-ray diffraction analysis, providing insights into the crystalline phases and crystal structure of the Sb<sub>2</sub>Se<sub>3</sub> films synthesized under different temperatures of the selenium source. The X-ray patterns exhibit distinct features, with notable observations regarding the intensity variations of specific peaks in response to increasing temperature of the selenium source. The X-ray diffraction patterns display prominent peaks corresponding to the crystallographic planes (221) and (211), indicating the presence of strong crystalline

phases. Additionally, peaks such as (020), (120), and (310), are also obviously in the X-ray patterns. Notably, these peak intensities demonstrate a dependence on the temperature of the selenium source, with alterations observed as the temperature increases. The selenium source temperature of  $T_{\text{Se}} = 370^\circ\text{C}$ , the XRD analysis reveals the disappearance of weak peaks, including (020), (120), (310), (230), (240), (002), and (320), while the strong peaks (221) and (211) remain raised. This suggests a distinct influence of the temperature on the crystal structure, leading to the elimination of certain crystallographic planes at temperatures up to  $T_{\text{Se}} = 370^\circ\text{C}$ . Furthermore, a subsequent increase in temperature to  $T_{\text{Se}} = 430^\circ\text{C}$  induces a decrease in the intensities of the (221) and (211) peaks, while the weak peaks (020), (120), (230), and (240) become significantly more pronounced. This temperature-dependent variation highlights the dynamic nature of the crystal structure and phase composition of the  $\text{Sb}_2\text{Se}_3$  films. Moreover, an additional observation is made at  $2\theta = 29.66^\circ$ , where a low-intensity reflex is detected in correspondence to the (101) peak. This reflex indicates the formation of the Se phase, providing evidence of a distinct phase transition or phase presence within the  $\text{Sb}_2\text{Se}_3$  films under the given experimental conditions. In summary, the XRD analysis of the  $\text{Sb}_2\text{Se}_3$  films elucidated valuable information regarding their crystal structure and phase composition. The obtained results demonstrate the influence of the selenium source temperature on the intensities of specific peaks, emphasizing the temperature-dependent alterations in the crystal structure. Additionally, the identification of the Se phase further contributes to the understanding of the film's structural properties.

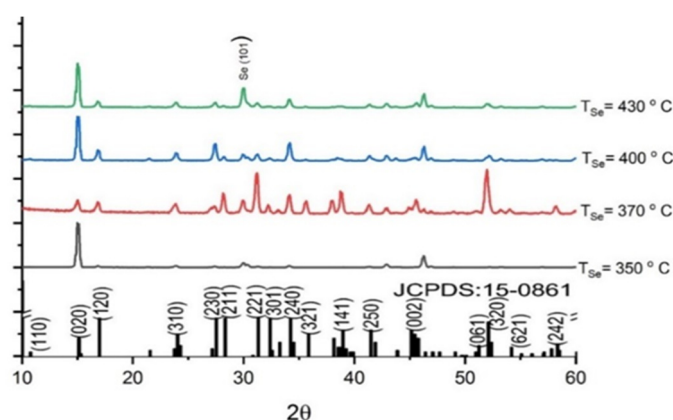


**Figure 3.** X-ray diffraction pattern of  $\text{Sb}_2\text{Se}_3$  films at different temperatures of the selenium source

To quantitate the orientation of  $\text{Sb}_2\text{Se}_3$  films, the texture coefficients ( $T_c$ ) of diffraction peaks were calculated based on the following equation [13]:

$$T_c = \frac{I_{(hkl)}}{I_{0(hkl)}} \left/ \left( \frac{1}{N} \sum_{i=1}^N \frac{I_{(h_i k_i l_i)}}{I_{0(h_i k_i l_i)}} \right) \right. \quad (1)$$

The intensities of the diffraction peaks, denoted as  $I_{(hkl)}$  and  $I_{0(hkl)}$ , respectively, correspond to the measured and standard X-ray diffraction patterns of  $\text{Sb}_2\text{Se}_3$  (JCPDS 15-0861) for the crystallographic planes (hkl). The determination of the peak intensity is crucial for analyzing the crystal orientation and structural properties of the material under investigation. Notably, the texture coefficient, TK, associated with the diffraction peaks signifies the level of orientation prevalence along a specific direction. In the case of the examined samples, the high TK values observed for the diffraction peaks indicate a pronounced orientation in the corresponding direction. Interestingly, at a selenium source temperature of  $370^\circ\text{C}$ , the TC values for crystallographic planes (hk0) in our samples tend to decrease. This initial decrease suggests a deviation from the dominant orientation, possibly due to the effect of elevated temperature on the crystal lattice arrangement. However, as the temperature of the selenium source continues to rise  $370^\circ\text{C}$ , a subsequent increase in the TK values for the (hk0) planes is observed. The temperature of the selenium source plays a significant role in influencing the crystal orientation and can result in distinct variations in the diffraction patterns of  $\text{Sb}_2\text{Se}_3$ . Further investigation is necessary to comprehensively understand the underlying mechanisms behind these observed temperature-dependent changes in crystal orientation and their implications for the materials properties.

#### 4. CONCLUSIONS

In this study, we investigated the effect of temperature on grain size and crystallographic orientation in selenium films. The results indicate that increasing the temperature of the selenium source leads to the formation of larger grains and the presence of rod-shaped grains of  $\text{Sb}_2\text{Se}_3$  aligned parallel to the substrate. The observed grain sizes and crystallographic orientations are in line with the collected data, as evidenced by the increased peak texture coefficients at the temperature of  $430^\circ\text{C}$ . These findings contribute to a better understanding of the growth mechanisms and properties of selenium films, which can aid in the development of tailored thin film technologies for various applications. Further studies exploring the influence of other parameters on grain formation and crystallographic orientation are warranted to expand our knowledge in this field. At a selenium source temperature of  $430^\circ\text{C}$ , large rod-like grains can be observed on

the surface of the  $Sb_2Se_3$  film.  $Sb_2Se_3$  films Se -deficient at a selenium source temperature of  $350^\circ C$ . As the temperature of the selenium source increases, the composition of the  $Sb_2Se_3$  film approaches stoichiometric.

#### Acknowledgment

The authors express their gratitude to Doctor of Physical and Mathematical Sciences, Professor T.M. Razikov for his assistance in conducting the experiments and discussing the results.

#### ORCID

- ✉ Takhirdjon M. Razikov, <https://orcid.org/0000-0001-9738-3308>;
- ✉ Zafarjon M. Khusanov, <https://orcid.org/0009-0005-9420-8033>
- ✉ Sultanpasha A. Muzafarova, <https://orcid.org/0000-0001-5491-7699>
- ✉ Ruhiddin T. Yuldoshov, <https://orcid.org/0000-0002-7886-1607>

#### REFERENCES

- [1] A. Mavlonov, T.M. Razykov, F. Raziq, J. Gan, J. Cantina, Yu. Kawano, T. Nishimura, et al., "A Review of  $Sb_2Se_3$  Photovoltaic Absorber Materials and Thin-Film Solar Cells," *Solar Energy*, **201**, 227 (2020). <https://doi.org/10.1016/j.solener.2020.03.009>
- [2] Y. Zhao, S. Wang, and C. Li, "Regulating deposition kinetics via a novel additive-assisted chemical bath deposition technology enables fabrication of 10.57%-efficiency  $Sb_2Se_3$  solar cells," *Energy Environ. Sci.* **15**, 5118-5128 (2022). <https://doi.org/10.1039/D2EE02261C>
- [3] C. Wang, S. Lu, S. Li, S. Wang, X. Lin, J. Zhang, R. Kondrotas, et al., "Efficiency improvement of flexible  $Sb_2Se_3$  solar cells with non-toxic buffer layer via interface engineering," *Nano Energy*, **71**, 104577 (2020). <https://doi.org/10.1016/j.nanoen.2020.104577>
- [4] Y. Zhou, L. Wang, S. Chen, S. Qin, X. Liu, J. Chen, D.-J. Xue, et al., *Nature Photonics*, **9**(6), 409-415 (2018). <https://doi.org/10.1038/nphoton.2015.78>
- [5] A. Shongalova, M.R. Correia, J.P. Teixeira, J.P. Leitão, J.C. González, S. Ranjbar, S. Garud, et al., "Growth of  $Sb_2Se_3$  thin films by selenization of RF sputtered binary precursors," *Sol. Energy Mater. Sol. Cells*, **187**, 219-226 (2018). <https://doi.org/10.1016/j.solmat.2018.08.003>
- [6] E.A. El-Sayad, "Compositional dependence of the optical properties of amorphous  $Sb_2Se_{3-x}S_x$  thin films," *Journal of Non-Crystalline Solids*, **354**(32), 3806-3811 (2008). <https://doi.org/10.1016/j.jnoncrysol.2008.05.004>
- [7] R. Kondrotas, J. Zhang, C. Wang, and J. Tang, "Growth mechanism of  $Sb_2Se_3$  thin films for photovoltaic application by vapor transport deposition," *Solar Energy Materials and Solar Cells*, **161**, 190-196 (2017). <https://doi.org/10.1016/j.solmat.2019.04.024>
- [8] X.X. Wen, C. Chen, S.C. Lu, K.H. Li, R. Kondrotas, Y. Zhao, W.H. Chen, et al., "Vapor transport deposition of antimony selenide thin film solar cells with 7.6% efficiency," *Nat. Commun.* **9**, 2179 (2018). <https://doi.org/10.1038/s41467-018-04634-6>
- [9] X.B. Hu, J.H. Tao, S.M. Chen, J.J. Xue, G.E. Weng, K. Jiang, Z.G. Hu, et al., "Improving the efficiency of  $Sb_2Se_3$  thin-film solar cells by post annealing treatment in vacuum condition," *Sol. Energy Mater. Sol. Cells*, **187**, 170-175 (2018). <https://doi.org/10.1016/j.solmat.2018.08.006>
- [10] D.B. Li, X.X. Yin, C.R. Grice, L. Guan, Z.N. Song, C.L. Wang, C. Chen, et al., "Stable and efficient  $CdS/Sb_2Se_3$  solar cells prepared by scalable close space sublimation," *Nano Energy*, **49**, 346-353 (2018). <https://doi.org/10.1016/j.nanoen.2018.04.044>
- [11] C.C. Yuan, X. Jin, G.S. Jiang, W.F. Liu, C.F. Zhu. " $Sb_2Se_3$  solar cells prepared with selenized dc-sputtered metallic precursors," *J. Mater. Sci: Mater. Electron.* **27**, 8906-8910 (2016). <https://doi.org/10.1007/s10854-016-4917-3>
- [12] S. Dias, B. Murali, and S.B. Krupanidhi, "Transport properties of solution processed  $Cu_2SnS_3/AlZnO$  heterostructure for low-cost photovoltaics," *Sol. Energy Mater. Sol. Cells*, **143**, 152-158 (2015). <https://doi.org/10.1016/j.solmat.2015.06.046>
- [13] F.I. Mustafa, S. Gupta, N. Goyal, and S. Tripathi, "Thin Films. In: Non-Ideal p-n junction Diode of  $Sb_{(x)}Se_{(1-x)}$  ( $x=0.4, 0.5, 0.6, 0.7$ ) Thin Films," *AIP Conference Proceedings*, **1393**, 75-76 (2011). <https://doi.org/10.1063/1.3653616>

#### ВИРОЩУВАННЯ ПЛІВОК $Sb_2Se_3$ , ЗБАГАЧЕНИХ СЕЛЕНОМ, ЗА ДОПОМОГОЮ ХІМІЧНОГО МОЛЕКУЛЯРНОГО ОСАДЖЕННЯ

Тахирджон М. Разіков, Султанпаша А. Музафарова, Рухіддін Т. Юлдошов, Зафарджон М. Хусанов, Маргуба К. Хусанова, З.С. Кенжаєва, Б.В. Ібрагімова

*Інститут фізики напівпровідників і мікроелектроніки Національного університету Узбекистану, 100057, Ташкент, Узбекистан, вул. Янги Алмазар, 20*

У цьому дослідженні вивчено ріст плівок  $Sb_2Se_3$  на поверхнях вапняно-натрієвого скла (SLG) за допомогою методу хімічного молекулярно-променевого осадження (СМРД) при температурі підкладки  $500^\circ C$ . Вихідними матеріалами для осадження плівок були використані високочисті бінарні сполуки  $Sb_2Se_3$  та Se. Для дослідження морфологічних характеристик плівок  $Sb_2Se_3$  використовували скануючу електронну мікроскопію (SEM). Крім того, було досліджено вплив температури на розмір зерен і кристалографічну орієнтацію в плівках селену. Зразки отримували з джерела селену при температурах  $370^\circ C$  і  $430^\circ C$ . Результати показують, що підвищення температури джерела селену призводить до утворення більших зерен і наявності стрижнеподібних зерен  $Sb_2Se_3$ , розташованих паралельно підкладці. Зразок, отриманий при  $370^\circ C$ , показав зерна розміром понад 2 мкм, рівномірно розподілені по поверхні підкладки, що свідчить про рівномірний процес росту. Навпаки, коли температуру джерела селену підняли до  $430^\circ C$ , на поверхні плівки підкладки були виявлені значно більші зерна розміром приблизно 4 мкм. Рентгеноструктурний аналіз був проведений, щоб отримати уявлення про кристалічні фази та кристалічну структуру плівок  $Sb_2Se_3$ , синтезованих за різних температур джерела селену. На рентгенівських дифракційних картинах відображені помітні піки, що відповідають кристалографічним площинам (221) і (211), що вказує на наявність сильних кристалічних фаз. Крім того, такі піки, як (020), (120) і (310), спостерігалися на рентгенівських картинах, що додатково підтверджує кристалічність плівок.

**Ключові слова:** рентгенівська дифракція; хімічне молекулярно-променево осадження;  $Sb_2Se_3$ ; температура селену